Received: 8 May 2023 | Accepted: 13 December 2023

DOI: 10.1002/nano.202300064

RESEARCH ARTICLE

nano select Open Access WILEY

Morphological design of PDVB-based particles

Silvia Freese[1] | **Gunnar Glasser**[2] | **Moritz Susewind**[3] | **Ingo Lieberwirth**[2] | **Thorsten Hofe**[3] | **Ulrich Jonas**[1]

[1]University of Siegen, Siegen, Germany

[2]Max-Planck Institute for Polymer Research, Mainz, Germany

[3]Polymer Standards Service GmbH, Mainz, Germany

Correspondence
Ulrich Jonas, University of Siegen, Adolf-Reichwein-Strasse 2, Siegen 57076, Germany.
Email: jonas@chemie.uni-siegen.de

Funding information
Zentrales Innovationsprogramm Mittelstand (ZIM) des Bundesministeriums für Wirtschaft und Energie (BMWi) FKZ ZF, Grant/Award Number: 4024604SL6

Abstract

Polymeric microspheres with complex architectures find application as stationary phases for size exclusion separation, solid supports for surface reactions, catalysis, and delivery systems. The microparticles are commonly made from divinylbenzene by precipitation polymerization or template swelling. Upon combining both methods and applying photopolymerization, we discovered new morphological features that are not solely explicable by the individual processes. Firstly, three types of templates were synthesized by precipitation polymerization: noncrosslinked, slightly crosslinked, and slightly crosslinked with noncrosslinked polystyrene fractions. All template types were swollen with divinylbenzene, which was polymerized by photoinitiation, followed by template extraction. Changes in particle size were tracked by light microscopy, while SEM revealed submicron features like hollow cores, toluene-insoluble walls, and surface grooves from the collapse upon drying of the toluene-swollen corona. Our investigations indicated that the corona results from chain transfer and crosslinking of the template during photoinitiation. Higher precrosslinking of the template reduced the core cavity volume of the extracted particle, while more mobile polystyrene chains led to larger cavities. These architectures are promising model systems for fundamental studies of particle interactions, aggregation, and structure formation in the field of colloidal physics.

KEYWORDS

colloidal template, free radical precipitation polymerization, particle architecture, particle swelling, PDVB, photoinitiation

1 | INTRODUCTION

Porous particles are an interesting class of materials for example in the field of size exclusion chromatography (SEC), sorbents, or delivery systems.[1]—[9] Typically, due to the larger volume demand in such applications, microspheres with dimensions in the 1–1000 micrometer range are favored over nanoparticles (approx. 1–100 nm).[10–12] Yet, the internal structural features enabling such advanced functionalities require the precise design of the particle nanoarchitecture.[13] A wide range of preparation methods for polymer particles exists which allow specific control over the particle size, morphology and architecture.[2,14–18] On the one hand, the particle size

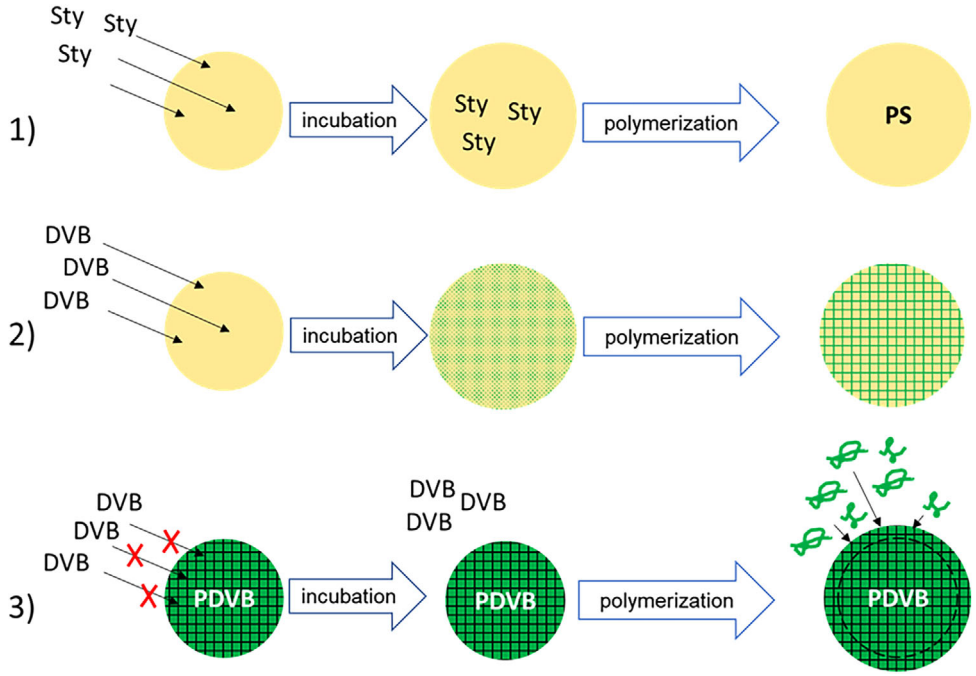

FIGURE 1 Comparison of precipitation mechanism versus swelling mechanism. Swelling of polystyrene (PS) particles with (1) styrene (Sty) or (2) divinylbenzene (DVB) and (3) precipitation of polydivinylbenzene (PDVB) chains on PDVB particles.

can be well tailored by precipitation polymerization[19] and emulsion polymerization.[20] On the other hand, a pore architecture can be introduced by suspension polymerization,[2,17,21] which results in polymer particles with a broad size dispersion, or by swelling of template particles with monomer retaining a narrow particle size distribution.[22] Figure 1 schematically shows the swelling method and precipitation polymerization technique that are commonly used to achieve specific particle sizes and morphologies for polystyrene (PS) and polyvinylbenzene (PDVB) systems.

Noncrosslinked polymer particles (like PS latex) are composed of single-chain entities and can be exploited as soluble template material for swelling with monomer followed by polymerization. By this procedure the particle size can be increased in a well-defined manner and pores can be introduced after dissolution of the template material when swelling with a crosslinking monomer.[1,22,23] In the literature, the emulsion polymerization technique is used for the preparation of the PS template with the disadvantage of the particle diameter being limited around 1 μm.[24] An extra step is needed to enlarge the particles after emulsion polymerization by swelling the PS matrix with additional styrene followed by polymerization (reaction pathway 1 in Figure 1). If DVB as crosslinking monomer is added to the noncrosslinked PS template particles, subsequent polymerization yields a PDVB network blended with mobile PS polymer chains inside the particle (pathway 2 in Figure 1). A concurrent phase separation of the PDVB network and the PS template may result in porous particles after dissolution of the PS template with a suitable solvent.[22,23] When performing precipitation polymerization with a crosslinking monomer like DVB, highly crosslinked particles are formed which do not swell with the monomer.[18] Further precipitation polymerization leads to shell growth by deposition of the newly formed polymer onto the particle surface (pathway 3 in Figure 1), whereby the shell is indistinguishable from the core.[19,25] In addition, various methods are reported in the literature[4,5,26] to achieve pore formation in fully crosslinked PDVB particles following pathway 3, yet with varying degrees of success.

The combination of such particle formation procedures appears attractive to exploit the advantages of the unique techniques and unite the architectural features attained with each method. Yet, such combinations do not necessarily lead to the expected properties which would result from the sum of the individual procedures, but indeed new properties may emerge from the interplay of the applied techniques.[27–31] Consequently, in this article we study the effect of combining precipitation polymerization and particle swelling on the resulting PDVB particle morphologies. Three different PDVB particle architectures originating from PS templates with varying crosslinking degrees are presented and the role of PS in the formation of grooves and pores is discussed.

2 | RESULTS AND DISCUSSION

2.1 | Preparation of crosslinked particles with grafted polystyrene chains (PDVB-gPS) from non-crosslinked seed templates (tPS^{nc})

A common route in precipitation polymerization to form a shell by changing the monomer and continuing the growth in a one-pot reaction, as mentioned above, was investigated here for the formation of a porous shell. Model experiments with toluene as a standard porogen did not yield discernible SEC separation behavior under our conditions (see Figures S1 to S11). Furthermore, using noncrosslinked PS as template material in such a precipitation polymerization in an attempt to generate a porous shell on a highly crosslinked core led to either agglomeration of the particles or the shell material remained in solution after the reaction. Thus, this route was deemed unsuitable to prepare porous shells (see also Figure S12). Following this unsuccessful attempt, we conceived three different strategies based on the combination of precipitation polymerization with template swelling.

As a first route, the above-described swelling method from the literature was implemented by swelling a noncrosslinked PS template particle with DVB, polymerize this crosslinker monomer, and remove the PS template by dissolution from the resulting PDVB network (Figure 2). In the literature,[24] this swelling process is performed with a noncrosslinked PS template, an excess of a monomer mixture (monomer mass : PS particle mass of 2:1 for an equal monomer mixture of Sty:DVB = 1:1), and the plasticizer dibutyl phthalate as swelling aid. The obtained spherical particles featured a diameter of 7.4 μm and a porous structure with a pore diameter average of 49 nm, when starting from a template with PS chains of molar mass $M_n = 4.1 \times 10^3$ g mol^{-1} and $M_w = 9.0 \times 10^3$ g mol^{-1}. With the aim of obtaining larger pores, the literature procedure was adapted by reducing the amount of DVB monomer with respect to PS template to 0.2:1 and completely excluding the styrene monomer. Since the lower monomer ratio requires less swelling of the template, the experiment was performed without the swelling aid. The morphological evolution with each subsequent process steps was followed by analysis of the particles after each process step. The particle dimensions were measured by light microscopy (LM), and, except for DVB swelling, scanning electron microscopy (SEM) was employed to investigate the surface morphology and inner pore structure after microtome sectioning.

In Figure 2A, the swelling procedure is schematically shown comprising. (1) Swelling of the template particle with a crosslinkable monomer and initiator, (2) photoinitiated polymerization of the monomer, and (3) extraction of the template polymer with a suitable solvent. Here, THF was chosen as solvent for these experiments. Noncrosslinked PS particles (in the following indicated as tPS^{nc}) from precipitation polymerization in ethanol served as templates (Figure 2B,E). Compared to the literature,[24] the preliminary swelling step with styrene to enlarge the particles is not necessary, since PS particles made by precipitation polymerization already have dimensions above 3 μm and a narrow size distribution below 10%. Poly-*N*-vinylpyrrolidone (PNVP) was employed as a stabilizing agent during the PS template synthesis and is apparently associated with the particles. This results in a hydrophilic surface. For the PNVP attachment to the particle two scenarios can be envisioned which may also coexist. Firstly, the PNVP chains may be entangled with the PS phase, or secondly, due to chain transfer reactions occurring at the PNVP backbone during the styrene precipitation polymerization, PS side chains are grafted onto the PNVP structure. Throughout this work, the resulting PNVP-rich phase is generally referred to as PNVP-co-PS. In our experiments we found that thermally induced polymerization with the DVB-swollen tPS^{nc} particles at 75°C leads to a broadening of the particle size distribution due to coalescence of the template particles. LM pictures and PSD diagrams of particles both from photoinitiated and temperature-initiated polymerizations are provided in Figure S13. Thus, for the preparation of the particle systems presented in this work, photoinitiation at room temperature was generally chosen to avoid temperature-induced coalescence. A photo of the setup for the photoinitiated polymerization is provided in Figure S17.

Comparison of the size distribution before and after swelling with DVB, as analyzed by LM (see Figure S14), indicated that the average particle size increased by 0.6 μm from 4.9 to 5.5 μm. When investigating the morphology before swelling, it was found that the tPS^{nc} particles display a smooth surface and a uniform inside without pores (Figure 2B). The stripes seen in the particles cross section in Figure 2E are cutting artifacts: the PS material is so soft that it gets deformed and torn at the cutting interface. After swelling with DVB and polymerization (resulting in the tPS^{nc}-PDVB particles), a granular particle structure is observed throughout the cross sections and on the particle surface (Figure 2C,F). Based on the crosslinking polymerization of DVB a semipenetrating PDVB network enclosing noncrosslinked PS chains is expected. Apparently, the formed network leads to a mechanically more robust particle with fewer cutting artifacts in the cross section compared to the tPS^{nc} particles. After removing the PS template with THF and drying the sample, crosslinked

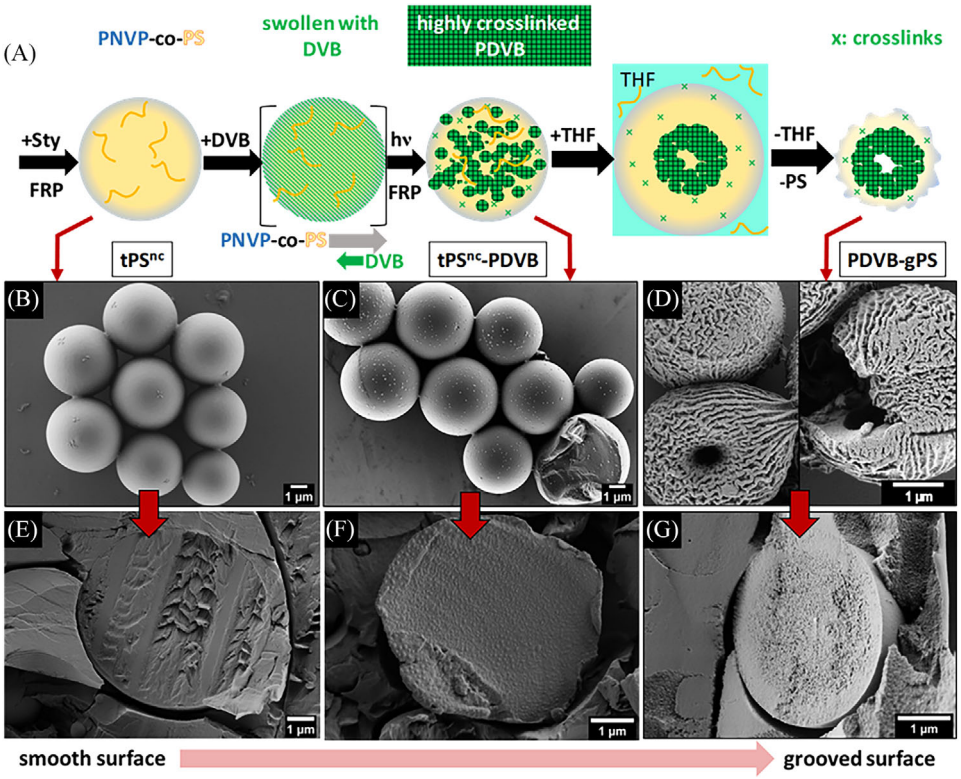

FIGURE 2 A, Three-step procedure involving the PS-template-swelling method and photoinitiation to prepare crosslinked particles with grafted polystyrene chains (PDVB-gPS) with a grooved surface. The green "x"s indicate crosslinks. SEM images of (B) noncrosslinked polystyrene template particles (tPS^{nc}) produced via precipitation polymerization (FRP: free radical polymerization) with PNVP-rich phases at the outer particle rim indicated as PNVP-co-PS above the tPS^{nc} particle, (C) PS particles with a semipenetrating network of PDVB inside (tPS^{nc}-PDVB), and (D) fully crosslinked PDVB particles after extraction of noncrosslinked PS chains (PDVB-gPS) – left: intact sphere (top) and indented particle (bottom) – right: fractured shell with hollow core visible. E–G, SEM images of particle cross sections.

particles with grafted polystyrene chains (PDVB-gPS) are obtained. The particle surface is characterized by deep grooves (Figure 3D), in contrast to the reported pore structure found in a similar fabrication process.[24] The top-view SEM images show three distinct particle morphologies, consisting in about 60%–70% of intact spheres, 30%–40% indented particles (both in Figure 2D left), and 5%–10% fractured shells (in Figure 3D right). This clearly documents the hollow nature of the particles after extraction. The ubiquitous existence of these three morphologies is unambiguously apparent in the two overview SEM images of Figure S19 and the particle gallery in Figure S20. The frequency of the different particle morphologies was determined by analysis of various overview SEM images with structural details of multiple particles clearly visible. As the deep indentations seen in Figures S18 to S20 appear only after the THF extraction step, they must result from the collapse of the hollow core after drying. The striking groove morphology found on the particle surface is particularly surprising, as such surface topology is not described for the particle architectures from similar preparation methods reported in the literature.[22,24,30,31] The cross section of a matrix-embedded PDVB-gPS particle (Figure 2G), however, shows a uniform pore structure in the core surrounded by a compact shell with few or no pores at all. For cross sectioning, the fragile particles need to be embedded in a matrix. The liquid resin used as matrix precursor has evidently penetrated the shell and filled the voids inside the particles. Consequently, after solidification and microtoming, details of the particle morphology entailing pores and a hollow core are hidden by the infused matrix.

To understand the morphological findings, various mechanisms discussed in the literature for this kind of particle preparation may be considered, with one of the prevalent processes being phase separation during swelling of the template particles.[30] During swelling with DVB and the photo-initiator, the PS chains are partially solvated, which increases their mobility. Based on previous literature reports, this leads to a phase separation of the following three components in the particle: The PNVP-rich phase (I) will stay at the particle-water interface due to the hydrophilic character of the PNVP chains,[27,29] while the similarly hydrophobic DVB (II) and PS (III)

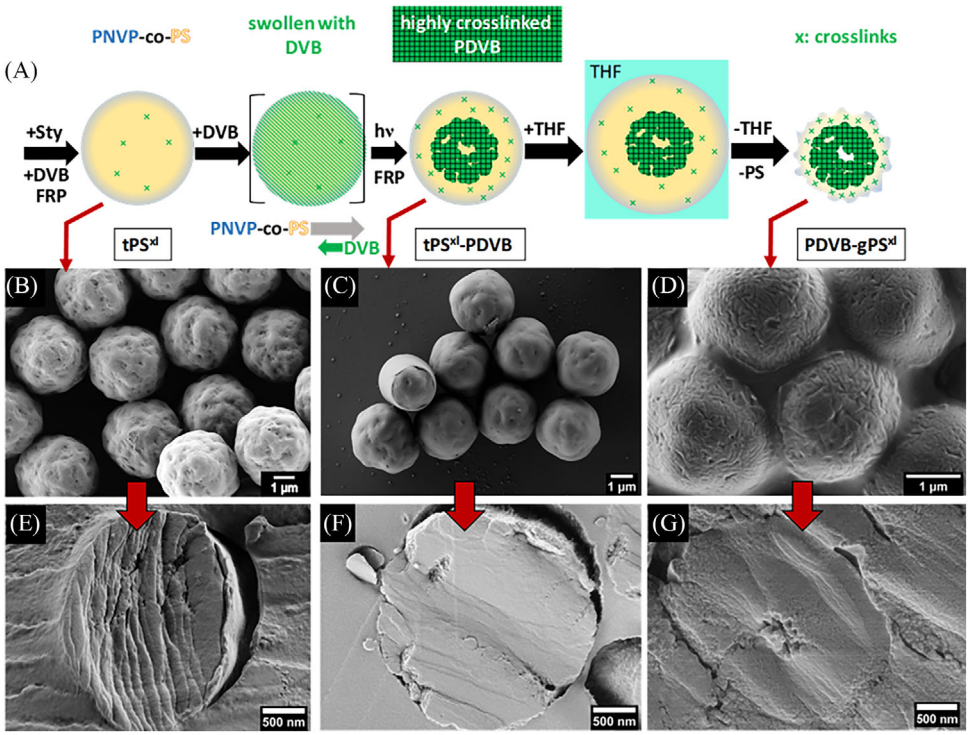

FIGURE 3 A, Three-step procedure involving the PS-template-swelling method and photoinitiation to prepare PDVB-gPS^{xl} particles from slightly crosslinked templates (tPS^{xl}). The green "x"s indicate crosslinks. SEM images of (B) slightly crosslinked PS template particles (tPS^{xl}) produced via precipitation polymerization (FRP: free radical polymerization) with PNVP-rich phases at the outer particle rim indicated as PNVP-co-PS above the tPS^{xl} particle, (C) PS particles with a semipenetrating network of PDVB inside (tPS^{xl}-PDVB), and (D) fully crosslinked PDVB particles after extraction of noncrosslinked PS chains (PDVB-gPS^{xl}). E–G, SEM images of particle cross sections.

fractions are expected to partition into the inner of the particle.[28] The localization of the individual phases is subsequently fixed during polymerization and concurrent crosslinking of the polymer chains. Thus, the PNVP-rich phase (I) can be assigned to the outermost section of the particle. The inner regions of the PDVB-gPS particles are rather inhomogeneous and show larger voids in the particle center after THF washing. These voids appear as large central indentations in the SEM images. Apparently, the DVB molecules (II) and the PS chains (III) behave differently during phase separation. Besides their similar hydrophobicity, the PS chains (III) accumulate more in the particle center compared to the formed PDVB network. This behavior was also found in other studies where PS particles were swollen with DVB.[30,31] According to the literature, phase separation effects increase with higher mobility of the involved species, which is relevant for the monomeric DVB (II) as well as for the PS chains (III).[28] DVB is a low-molar-mass liquid before polymerization with high mobility. It enters from outside of the particles and diffuses through the PS template inwards. This leads to a concentration gradient with higher concentration at the outer region of the core and dropping towards the center. Yet, it also plasticizes the PS chains that consequently attain higher mobility. Similarly, the initiator molecules dissolved in the DVB phase enter from the outside through the particle surface and diffuse into the PS matrix. Upon initiation by UV irradiation, DVB molecules react via a free radical chain growth mechanism to form a PDVB network with significantly reduced translational mobility, as the network expands. Thus, monomer addition to the radical sites at the network periphery can only proceed by reaction diffusion of the monomer to the network.[32] In this diffusion process, a PS chain localized next to the reaction center exchanges its position with an approaching DVB molecule that subsequently adds to the network, by which it grows. Consequently, by this mechanism the PS template is displaced by the newly formed PDVB material. As the light intensity and potentially also the initiator concentration is highest at the particle surface and decreasing inwards, PDVB network formation is expected to predominantly engage from the outer region of the tPS^{nc} particles and progress towards the center. This leads to an accumulated PS phase in the core. As a result, the crosslinking polymerization yields a shell of a PDVB-rich network around a PS-rich core. In this process, the PDVB phase may also grow around single PS chains, forming a semipenetrating network. After THF extraction of the mobile PS chains, a hollow core remains in the particle center. The grooves found on the PDVB-

gPS particles after solvent extraction with THF most likely derive from the drying process of the THF-saturated particle indicating a highly swollen outer shell. As the PDVB network is highly crosslinked, it cannot display such a high swelling ratio. On the other hand, the noncrosslinked PS chains are expected to completely dissolve in the THF phase. Yet, a weakly crosslinked network as prerequisite for the highly swollen shell must entail longer chain segments between the crosslinks that can only be provided by the PS template. The required crosslinks may have formed as a result of chain transfer reactions at the PS backbones during the free radical polymerization of the PDVB network. As this occurs throughout the whole PS phase, a weakly crosslinked PS network coexists with noncrosslinked PS chains in the resulting PDVB-gPS particle. This weakly crosslinked PS network is permanently jointed with the higher crosslinked PDVB phase. Thus, we refer to it as a grafted PS network, in short "gPS" for the particle acronym. In a good solvent like THF, the weakly crosslinked PS shell and the PNVP-rich outer phase will swell to a gel corona around the particle. Upon drying the corona folds down into a convoluted structure with grooves on the PDVB-gPS particle surface. The existence of such a swollen gel corona around the particles in a good solvent is corroborated by the difficulties of column packing during the SEC experiments. The PDVB-gPS particles could be well loaded into a SEC column when dispersed in a more polar solvent, like acetone. But upon solvent exchange to THF as good solvent for PS, the backpressure of the column increased drastically due to blocking of the interstitial volume by the THF-swollen corona. Rupturing of the particles by the applied pressure could be excluded since the particles were still intact after extraction from the column. Based on this evidence, the PDVB-gPS particles were considered not suitable as SEC stationary phase for organic solvents that swell PS (but this may be different for SEC in aqueous media). Yet, a further indication for the PS gel corona becomes evident upon the unsuccessful attempt to redisperse the dried PDVB-gPS particles in ethanol after THF extraction and drying, while the tPS^{nc}-PDVB particles could be well dispersed in ethanol before the extraction step. Such behavior can be explained by the coalescence of the swollen PS gel corona between particles that leads to agglomeration by chain entanglement upon drying (visible by the capillary necks between the particles shown in Figure S18, middle image, bottom row in the Supporting information).

The above set of experimental results effectively demonstrates how a complex property profile results from the combination of the two different procedures, that is, precipitation polymerization and template swelling. As such, this method provides access to microparticles with a hollow core, a hard shell, and a very soft corona when suspended in a good solvent for PS, as well as an intricate surface topography after drying.

2.2 | Crosslinked particles with grafted polystyrene chains (PDVB-gPS^{xl}) from slightly crosslinked seed templates (tPS^{xl})

In an attempt to suppress the gel corona formation, the above-described procedure was modified by introducing a low crosslink density in the PS template particles. While a higher crosslink density in the template would be advantageous to suppress such a gel corona more effectively, it would hamper sufficient swelling with DVB. Thus, a weak crosslink density with around 5% network junctions connecting the linear PS chain segments was targeted.

For the successful synthesis of the tPS^{xl} template particles, a maximum volume ratio of 4:96 v/v DVB:Sty was employed for precipitation polymerization of styrene in ethanol. Higher DVB ratios resulted in excessive particle agglomeration. The resulting, slightly crosslinked tPS^{xl} template particles were subjected to the same swelling process as presented above for the tPS^{nc} particles. The schematic mechanism and SEM images illustrating the particle morphologies resulting from the different reaction stages are shown in Figure 3.

The slightly crosslinked template particles tPS^{xl} in Figure 3B show a much more irregular shape compared to the noncrosslinked tPS^{nc} templates. The tPS^{xl} surface exhibits an irregular topography with corrugations leaning to a raspberry-like appearance. The microtome cutting (Figure 3E) reveals a rather compact particle and only a slight hint of a porous structure, but as above for tPS^{nc} particles, potential filling of the pores with the matrix material cannot be excluded. The diameter of the tPS^{xl}-PDVB particles increased by about 0.4 μm after swelling of the tPS^{xl} particles with DVB and polymerization. Light microscope data on particle size distribution and swelling can be found in Figure S15. Compared to the noncrosslinked tPS^{nc} particles, the size increase observed here after swelling is smaller due to the precrosslinking of the tPS^{xl} template. The dimensions and the size distribution are retained between swelling and photopolymerization, as it was previously observed with the tPS^{nc} particles. The tPS^{xl}-PDVB particle topography appears flattened out in the SEM images (Figure 3C) after swelling and subsequent polymerization, yet, they are more irregular than the spherical tPS^{nc}-PDVB particles in the first approach above (Figure 2C). The SEM cross sections in Figure 3F show a uniform particle morphology without any differences between phases. Again, some indication of a pore structure may be perceived, but particle penetration with the matrix material during the microtome

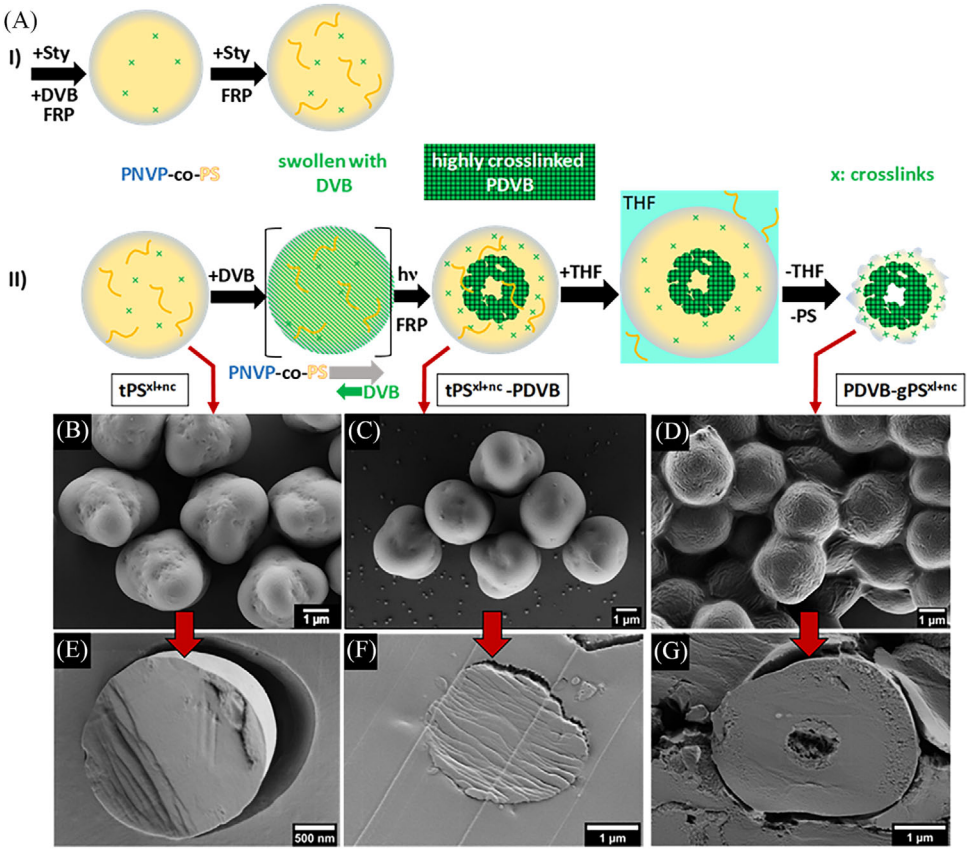

FIGURE 4 Schematics of (A-I) the procedure for tPS^{xl} template modification by further swelling with styrene and subsequent thermally initiated free radical polymerization (FRP) to form tPS^{xl+nc} templates and (A-II) the three-step procedure involving the PS-template-swelling method and photoinitiation to prepare PDVB-gPS^{xl+nc} particles from tPS^{xl+nc} templates. The green "x"s indicate crosslinks. SEM images of (B) slightly crosslinked PS template particles (tPS^{xl+nc}) produced via precipitation polymerization (by FRP) with PNVP-rich phases at the outer particle rim indicated as PNVP-co-PS above the tPS^{xl+nc} particle, (C) PS particles with a semipenetrating network of PDVB inside (tPS^{xl+nc}-PDVB), and (D) fully crosslinked PDVB particles after extraction of mobile PS chains (PDVB-gPS^{xl+nc}). E–G, SEM images of respective particle cross sections.

embedding step may have occurred. The removal of the PS template with THF results in PDVB-gPS^{xl} particles with a grooved surface and a granular inner particle structure and a central void (Figure 3D,G). It is important to note that the cross-sectional SEM investigations were performed on a dried sample that was microtome-sectioned without matrix embedding. In contrast to the samples above, the present particles were mechanically robust enough to be sectioned without matrix. Compared to the PDVB-gPS particles from the first approach (Figure 2D), the surface grooves of the PDVB-gPS^{xl} sample are much less pronounced. The particles are covered by a diffuse layer and the interstitial space is filled with a homogeneous phase interconnecting the individual spheres. In the SEM overview images, no characteristic indentations are visible for the PDVB-gPS^{xl} particles in contrast to the deep indentations frequently observed for the PDVB-gPS particles above. However, in the cross-section images of Figure 4G smaller, granule-filled voids are found in the PDVB-gPS^{xl} particle cores (compare also Figure S7). No embedding procedure prior to microtome cutting was applied to these PDVB-gPS^{xl} samples, so matrix infusion is excluded, and the internal particle morphology can be observed more clearly. More examples of the particles with voids are provided in Figure S22.

The phase separation mechanisms for the PDVB-gPS particles above also apply for the explanation of the morphological features obtained with the PDVB-gPS^{xl} particles here. Yet, as major difference, the precrosslinking of the tPS^{xl} templates substantially reduces PS chain mobility and thus affects the details of the PS phase separation upon PDVB network formation. Consequently, less PS material accumulates in the particle center and results in a smaller void volume after THF extraction. As discussed for the PDVB-gPS particles above, radical chain transfer takes place during the DVB polymerization step. This now generates additional crosslinks in the precrosslinked tPS^{xl} template. The gel corona with a higher crosslinking degree

swells less in THF and forms less distinct surface folds upon drying compared to the PDVB-gPS sample. The dried corona acts like a diffuse layer that covers up smaller surface details and forms interconnecting necks between the particles. More PS chain segments remain bound to the PDVB-gPS^{xl} particles after washing with THF because of the higher crosslink density compared to the PDVB-gPS particles. The participation of remaining free PS chains in the formation of the diffuse surface layer can be excluded, since Soxhlet extraction over 2 days was employed for the washing process. Ergo, the PDVB-gPS^{xl} system is not suitable as SEC stationary phase for PS solvents (like THF), as the soft, swollen corona fills the interstitial volume and blocks the SEC column. By employing template PS particles that are lightly crosslinked, the resulting particle morphology from this second approach are characterized by a rather smooth surface and less free volume in the core. Thus, they are very distinct from the particles of the first approach starting from noncrosslinked PS templates. These experimental findings document that the resulting PDVB particle morphology may be tailored by tuning the crosslinking density in the PS template.

2.3 | Crosslinked particles with grafted polystyrene chains (PDVB-gPS^{xl+nc}) from slightly crosslinked seed templates containing additional mobile chains (tPS^{xl+nc})

Since the two approaches above provide very different particle structures, we further investigated a third strategy that combines the crosslinked PS templates with mobile PS chains. The process started with swelling the slightly crosslinked tPS^{xl} template particles from the second approach with styrene followed by thermally initiated free radical polymerization (Figure 4A-I). This introduces noncrosslinked PS chains into the PS^{xl} matrix. The resulting composite PS^{xl+nc} template particles were subjected to DVB swelling (Figure 4A-II). While retaining the absolute number of crosslinks compared to the tPS^{xl} templates from the second approach, now additional mobile PS chains are incorporated into the particle. This should lead to more free volume in the particle after THF extraction of the mobile PS chains.

In Figure 4B–G, the SEM images show different stages of the process leading to the PDVB-gPS^{xl+nc} particles from the third strategy.

The SEM images of the tPS^{xl+nc} template particles show less corrugations (Figure 4B) than the tPS^{xl} templates (Figure 3B). Further swelling with DVB and subsequent polymerization smoothens those corrugations even more (Figure 4C). The cross-sections of both particle types show homogeneous bulk particles without voids or pores (Figure 4E,F). However, as indicated for the tPS^{nc} and tPS^{nc}-PDVB particles, matrix embedding for microtome sectioning might cause filling of potentially existing granular or porous structures, so that they are indiscernible here. An overall size increase of about 0.2 μm can be observed in light microscopy during DVB swelling (see Figure S16) with the particle dimensions being retained during polymerization. After the template extraction step, the PDVB-gPS^{xl+nc} particles possess a grooved surface (Figure 4D) similar to the topography of the PDVB-gPS^{xl} particles, yet the surface features are less distinctive than for the PDVB-gPS samples from the first strategy. Consequently, the introduction of additional mobile PS chains in the template did not significantly affect the swelling behavior of the gel corona. Apparently, the primary parameter influencing corona swelling is the absolute number of crosslinks in the template particle, here provided by the tPS^{xl} system. Due to the existence of a swellable corona, also these PDVB-gPS^{xl+nc} particles are not suitable as SEC stationary phase with a PS solvent. In the dry state, the corona interconnects and covers the PDVB-gPS^{xl+nc} particles, comparable to the PDVB-gPS^{xl} particles from the second strategy above. The SEM image with the particle cross section (Figure 4G) reveals a large cavity with micrometer dimensions in the particle center reminiscent of the smaller, granule-filled voids found in the PDVB-gPS^{xl} particles (Figure 3G). The wall of the voids is formed by distinctive granules with diameters below 100 nm (Figure S28), resulting in a porous structure, yet with more free volume compared to PDVB-gPS^{xl}. The gallery in Figure S24 shows a collection of cross-sectional SEM images with the voids. In the cross section of Figure 4G, a porous region of about 0.6 μm thickness is visible at the outer shell of the PDVB-gPS^{xl+nc} particles. The 0.9 μm thick region in between the center void and the outer porous shell is dense without pores. The void volume of the PDVB-gPS^{xl+nc} particles is larger than then one of PDVB-gPS^{xl} particles and can be explained by the dissolution of the additional mobile PS chains in the template. This observation is based on the SEM images of Figure S26.

From the comparison of the morphological findings for the PDVB-gPS^{xl+nc} particles (third strategy) and the PDVB-gPS^{xl} particles (second strategy), it becomes apparent that the void volume in particle cores can be directly controlled via the inclusion of mobile PS chains in slightly crosslinked templates.

3 | CONCLUSION

In this work, we merged precipitation polymerization with particle swelling and photopolymerization methods

into three distinct strategies, yielding intricate colloid architectures. The first approach utilized noncrosslinked polystyrene template particles, leading to PDVB-gPS particles with remarkable surface grooves and a hollow core. This is not expected when swelling a noncrosslinked template PS particle prepared by precipitation polymerization. The second strategy involved slightly crosslinked PS templates, resulting in shallower grooves and reduced core voids due to template crosslinking. The third strategy introduced mobile PS chains within slightly crosslinked PS templates, increasing the hollow core volume in the final microspheres. These findings demonstrate the ability to tailor void sizes in two opposing ways, highlighting the versatility of our approach. While SEM analysis allowed the detailed observation of various morphological features, we found that embedding the particles into a matrix for microtome cutting may have obscured some internal morphology for nonextracted particles. As a result, we refrained from embedding and instead used compact dried films of the extracted particles for sectioning. Consequently, more nanoscopic details of the morphology could be successfully visualized by SEM.

The unique combination of preparation methods for the microspheres with a soft corona, a robust shell, and a hollow core provides access to various applications such as size exclusion separation, surface reactions, catalysis, and delivery systems. Furthermore, these advanced colloidal architectures, achievable through tailored templating and swelling, hold promise as model systems for studying particle interactions, aggregation, and structure formation in the field of colloidal physics. As this work is a proof of concept with a limited set of parameter variations, future research could provide further insights to gain an extended control over the nanoarchitecture, potentially expanding to other templating methods.

4 | EXPERIMENTAL SECTION

4.1 | Chemicals

AIBN (azobis(isobutyronitril), 98.0%, Fluka Analytical), ACN (acetonitrile, 99.9%, Chemsolute), BAPO (Bis(2,4,6-trimethylbenzoyl)-phenylphosphineoxide, also known as Irgacure 819, Acrylat Shop), DVB (divinylbenzene, stab., 60.0%–65.0%, 34.0%–39.0% ethylvinyl benzene, Merck), ethanol (absolute, 99.98%, VWR chemicals), Methocel (K100, methyl cellulose), PNVP (polyvinylpyrrolidone, M_w = 40 000 g mol^{-1}, Alfa Aesar), styrene (stab., 99%, Alfa Aesar) and water. All chemicals were used as received.

4.2 | PS template particles

4.2.1 | Noncrosslinked PS^{nc} template

Adapted from literature,[33] noncrosslinked PS particles were prepared as follows: styrene (8.3v% of the total reaction volume), PNVP (M_w = 40 000 g mol^{-1}, 25 mol% wrt. monomer content) and AIBN (3 mol% wrt. to monomer content) were dissolved in ethanol (absolute, 91.7v% of the total reaction volume) in a round bottom flask. In a preheated oil bath, the reaction was carried out at 75°C for 20 hours at a stirring speed of 130 rpm. For purification, the particles were centrifuged and the supernatant liquid was replaced by fresh ethanol. This step was repeated at least 5 times before the particles were dried under ambient conditions for 24 hours.

4.2.2 | Slightly crosslinked PS^{xl} template

The procedure for PS^{xl} template particles was carried out in the same way as the procedure for noncrosslinked PS template particles but with a mixture of styrene and DVB (Sty:DVB 96:4 v/v) instead of neat styrene.

4.2.3 | Combined PS^{xl+nc} template

PS^{xl} template particles were dispersed in a solution consisting of ethanol (absolute, 99v% of total volume), styrene (4v% of total volume, PS:Sty = 1:1), PNVP (M_w = 40 000 g mol^{-1}, 50 mol% wrt. PS particles) and AIBN (3 mol% wrt. to monomer) and stirred for 2 hours at room temperature. The reaction was carried out in a preheated oil bath at 75°C for 20 hours at a stirring speed of 130 rpm. For purification, the particles were centrifuged and the supernatant liquid was replaced by fresh ethanol. This step was repeated at least 5 times before the particles were dried under ambient conditions for 24 hours.

4.3 | PDVB particles via PS template particles: PDVB-gPS, PDVB-gPS^{xl}, and PDVB-gPS^{xl+nc}

PS template particles (see Table 1, 300 mg) were evenly dispersed in an aqueous Methocel solution (18.6 g L^{-1}, 7.5 mL) before a solution of DVB (65 µL, 60 mg; PS:DVB 5:1 wt) and Irgacure 819 (6 mol% wrt. monomer, 11.5 mg) in ethanol (1 mL) was added dropwise under fast stirring at 0°C. To ensure a stable dispersion, the mixture was stirred for 2 hours under aforementioned conditions and then stored

TABLE 1 Details about the particle types used in the three different preparation methods to obtain the product particles PDVB-gPS, PDVB-gPS^{xl}, and PDVB-gPS^{xl+nc}, with the particle diameter of different reaction stages measured using pictures from light microscopy (template and monomer swollen particle dispersed in the reaction medium) and SEM (dried particles after THF extraction).

Product particle	Template particle	Template particle diameter/± 0.1 µm	Swollen template diameter/± 0.1 µm	Dried particle diameters after THF extraction
PDVB-gPS	tPS^{nc}	4.9 µm	5.5 µm	2.8–3.1 µm
PDVB-gPS^{xl}	tPS^{xl}	3.3 µm	3.7 µm	2.8–3.1 µm
PDVB-gPS^{xl+nc}	tPS^{xl+nc}	3.7 µm	3.9 µm	2.6–2.9 µm

overnight at 7°C without stirring. After the mixture was irradiated under mild stirring for 1 hour (Nichia UV LED lamp NVSU333A 365 nm, 3.64 W; mode: 4.2 V, 3.8 A), it was slowly stirred under light exclusion at room temperature for additional 20 hours.

For purification, the particles were centrifuged and the supernatant liquid was replaced by water. This step was repeated at least 5 times or until the supernatant liquid was as viscous as water. The same process was repeated once each with ethanol:water 1:3, 1:1, 3:1 and ethanol before the particles were dried under ambient conditions for 24 hours.

The template extraction with THF was carried out in a Soxhlet extractor for 2 days.

4.4 | Light microscopy and particle size analysis

Light microscopy was performed with a Zeiss Axioskop 50 microscope and a bresser MikroCam SP 3.1 camera (Software: MikroCamLabII version 3.7.13814.20190120 (64 bit)). Bright field transillumination was used for all shown LM pictures. Used objectives were a.) Zeiss Epiplan–Neofluar 50x magnification with NA = 0.75. The resulting images were processed with ImageJ version 1.52i (running with Java 1.8.0_271 (64 bit)). Scaling was done with a microscope slide with a micrometer scale standard.

4.5 | Scanning electron microscopy (SEM)

For SEM measurements of the particles, a drop of the sample dispersion was dropped onto a silicon wafer and allowed to dry under ambient conditions. Without further coating of the sample, it was examined using a LEO Gemini 1530 (Zeiss, Oberkochen, Germany) at a probe current between 15 and 70 pA at an accelerating voltage of 700 V. To prepare the cross sections, several drops of the sample dispersion were dropped onto a cured Epofix (Agar Scientific, Stansted, UK) substrate. After complete drying, another layer of Epofix was applied and cured. The resin-embedded particles were cut into 2 µm thick sections in an ultramicrotome (UCT 7, Leica, Germany) using a diamond knife (Diatome, Switzerland) and then transferred to a silicon wafer. SEM examination of the cross sections was performed in LEO Gemini 1530 under the same conditions as indicated above.

ACKNOWLEDGMENTS

This project was founded by Zentrales Innovationsprogramm Mittelstand (ZIM) des Bundesministeriums für Wirtschaft und Energie (BMWi) FKZ ZF 4024604SL6.

Open access funding enabled and organized by Projekt DEAL.

CONFLICT OF INTEREST STATEMENT

The authors declare no conflicts of interest.

DATA AVAILABILITY STATEMENT

Data is available on request.

REFERENCES

1. Galia, M., Svec, F., Frechet, J. M. J., *J. Polym. Sci. Part Polym. Chem.* **1994**, *32*, 2169.
2. Lubomirsky, E., Khodabandeh, A., Preis, J., Susewind, M., Hofe, T., Hilder, E. F., Arrua, R. D., *Anal. Chim. Acta* **2021**, *1151*, 338244.
3. Li, W.-H., Stöver, H. D. H., Hamielec, A. E., *J. Polym. Sci. Part Polym. Chem.* **1994**, *32*, 2029
4. Li, W.-H., Stöver, H. D. H., *J. Polym. Sci. Part Polym. Chem.* **1998**, *36*, 1543
5. Perrier-Cornet, R., Héroguez, V., Thienpont, A., Babot, O., Toupance, T., *J. Chromatogr. A* **2008**, *1179*, 2.
6. Tennikova, T. B., Horák, D., Švec, F., Tennikov, M. B., Kever, E. E., Belenkii, B. G., *J. Chromatogr. A* **1989**, *475*, 187.
7. Beltran, A., Borrull, F., Marcé, R. M., Cormack, P. A. G., *TrAC Trends Anal. Chem.* **2010**, *29*, 1363
8. Oladele, I. O., Onuh, L. N., Agbeboh, N. I., Alewi, D. D., Lephuthing, S. S., *Nano Sel.* **2023**, *4*, 419.
9. Yazdanpanah, A. Ghaffari, M., Ahmadi, Z., Abrishamkar, A. B., Sattarzadeh, S., Ramedani, A., Arabyazdi, S., Moztarzadeh, F., *Nano Sel.* **2023**, *4*, 353.
10. Mahale, M. M., Saudagar, R. B., *J. Drug Deliv. Ther.* **2019**, *9*, 854.
11. Cai, Y., Chen, Y., Hong, X., Liu, Z., Yuan, W., *Int. J. Nanomedicine* **2013**, *8*, 1111.

12. Sahil, K., Akanksha, M., Premjeet Singh, S., Bilandi, A., Kapoor, B., *Int. J. Res. Pharm. Chem.* **2011**, *1*.
13. Mekuye, B., Abera, B., *Nano Sel.* **2023**, *4*, 486.
14. Ramli, R. A., Laftah, W. A., Hashim, S., *RSC Adv.* **2013**, *3*, 15543.
15. Gokmen, M. T., Du Prez, F. E., *Prog. Polym. Sci.* **2012**, *37*, 365.
16. Yabu, H., *Polym. J.* **2013**, *45*, 261.
17. Okay, O., *Prog. Polym. Sci.* **2000**, *25*, 711.
18. Li, K., Stöver, H. D. H., *J. Polym. Sci. Part Polym. Chem.* **1993**, *31*, 3257.
19. Downey, J., Stöver, H. D. H. Growth Mechanism of Poly(divinylbenzene) Microspheres in Precipitation Polymerization—Macromolecules (ACS Publications). https://pubs.acs.org/doi/10.1021/ma9812027
20. Sm̆igol, V., Sv̆ec, F., Hosoya, K., Wang, Q., Fréchet, J. M. J., *Angew. Makromol. Chem.* **1992**, *195*, 151.
21. Seidl, J., Malinský, J., Dušek, K., Heitz, W., in *Fortschritte der Hochpolymeren-Forschung* (Ed. J. H. Winter), Springer, **1967**, p. 113.
22. Wang, Q. Ching., Hosoya, Ken., Svec, Frantisek., Frechet, J. M. J., *Anal. Chem.* **1992**, *64*, 1232.
23. Frechet, J. M. J., Svec, F. Column with Microporous Polymer Media, US19910779929, **1993**.
24. Wang, Q. C., Švec, F., Fréchet, J. M. J., *J. Polym. Sci. Part Polym. Chem.* **1994**, *32*, 2577.
25. Li, W.-H., Stöver, H. D. H., *Macromolecules* **2000**, *33*, 4354.
26. Limé, F., Irgum, K., *Macromolecules* **2009**, *42*, 4436.
27. Kirsch, S., Doerk, A., Bartsch, E., Sillescu, H., Landfester, K., Spiess, H. W., Maechtle, W., *Macromolecules* **1999**, *32*, 4508.
28. Lee, D. I., Ishikawa, T., *J. Polym. Sci. Polym. Chem. Ed.* **1983**, *21*, 147.
29. Lee, S., Rudin, A., *J. Polym. Sci. Part Polym. Chem.* **1992**, *30*, 865.
30. Okubo, M., Minami, H., *Colloid Polym. Sci.* **1997**, *275*, 992.
31. Minami, H., Kobayashi, H., Okubo, M., *Langmuir* **2005**, *21*, 5655.
32. Young, R. J., Lovell, P. A. *Introduction to Polymers*, 3rd ed., CRC Press, **2011**.
33. Almog, Y., Reich, S., Levy, M., *Br. Polym. J.* **1982**, *14*, 131.

SUPPORTING INFORMATION

Additional supporting information can be found online in the Supporting Information section at the end of this article.

How to cite this article: S. Freese, G. Glasser, M. Susewind, I. Lieberwirth, T. Hofe, U. Jonas, *Nano Select* **2024**, *5,* 2300064.
https://doi.org/10.1002/nano.202300064